Original Paper

Cells Tissues Organs

Cells Tissues Organs
DOI: 10.1159/000348617

Accepted after revision: February 4, 2013
Published online: May 4, 2103

Immunoreactive Endothelin-1 and Endothelin A Receptor in Basilar Artery Perivascular Nerves of Young and Adult Capybaras

Andrzej Loesch[a] Michael R. Dashwood[b] Antonio A. Coppi[c]

[a]Division of Medicine and [b]Department of Clinical Biochemistry, University College London Medical School, London, UK; [c]Laboratory of Stochastic Stereology and Chemical Anatomy, Department of Surgery (LSSCA), College of Veterinary Medicine, University of São Paulo, São Paulo, Brazil

Key Words
Basilar artery · Endothelin · Endothelin A receptor · Perivascular nerves · Synaptophysin · Capybara

Abstract
The purpose of this qualitative morphological study was the immunocytochemical and ultrastructural comparison of perivascular nerves of the basilar artery (BA) of young (6-month-old) and adult (12-month-old) capybaras – adult capybaras showed regression of the internal carotid artery (ICA). The study focused on immunolabeling for the vasoactive peptide endothelin-1 (ET-1) and endothelin A receptor (ET_A) as well as for the synapse marker synaptophysin (SYP). In the BA of young capybaras, immunoreactivity for ET-1, ET_A receptor and SYP was detected in perivascular nerve varicosities and/or intervaricosities. Immunoreactivity for ET-1 and ET_A receptor was also displayed by some Schwann cells, which accompanied perivascular nerves. In addition to the presence of the above-described perivascular nerve characteristics, the BA of adult animals also revealed structurally altered perivascular nerves, where axon profiles were irregular in shape with dense axoplasm, while the cytoplasm of Schwann cells was vacuolated and contained myelin-like figures. These structurally altered perivascular nerves displayed immunoreactivity for ET-1, ET_A receptor and SYP. These results show that the ET-1 system is present in some of the BA perivascular nerves and it is likely that this system is affected during animal maturation when ICA regression takes place. The role of ET-1 in cerebrovascular nerves is still unclear but its involvement in neural (sensory) control of cerebral blood flow and nerve function is possible.

Introduction

The capybara, *Hydrochaeris hydrochaeris* [Herrera and Macdonald, 1984], is the largest living rodent. It lives wild in swamp areas of South American countries, including Argentina, Brazil and Colombia, and is also

Abbreviations used in this paper

BA	basilar artery
EM-I	immunocytochemistry at electron-microscopic level
ET-1	endothelin-1
ET_A	endothelin A receptor
ET_B	endothelin B receptor
ICA	internal carotid artery
NGS	normal goat serum
NHS	normal horse serum
PBS	phosphate-buffered saline
SYP	synaptophysin
TEM	transmission electron microscopy

KARGER

E-Mail karger@karger.com
www.karger.com/cto

1422–6405/13/0000–0000$38.00/0

Prof. A. Loesch
Division of Medicine, University College London Medical School
Royal Free Campus, Rowland Hill Street
London NW3 2PF (UK)
E-Mail a.loesch@ucl.ac.uk

farmed for meat and skin. Its life span in the wild is around 10–14 years. Young and adult animals are considered to be 6 and 12 months, respectively [Herrera and McDonald, 1984]. Anatomical study of capybara showed that the internal carotid artery (ICA) and the basilar artery (BA) are essential for the blood supply to the capybara brain [De Vriese, 1905; Reckziegel et al., 2001]. At maturation, at around 1 year of age, ICA regression can be observed in this species [Reckziegel et al., 2001], suggesting that from this stage the main blood supply to the capybara brain is via the BA of the vertebrobasilar system. Morphological features suggesting BA remodeling in capybara during ICA regression have been described [Islam et al., 2004; Steele et al., 2006].

In mammals, including laboratory rodents, the autonomic innervation of the cerebral arteries is fairly well described as is the well-established role of a number of vasoactive factors: neurotransmitters, cotransmitters and/or neuromodulators in sympathetic, parasympathetic and sensory nerves participating in the control of cerebral blood flow [Burnstock, 1988, 1990; Ralevic and Burnstock, 1993; Faraci and Brian, 1994; Saetrum Opgaard et al., 1998]. Less is known regarding the presence and role of ET-1 and its receptors in cerebrovascular nerves [Loesch et al., 1998, 2005]. So far, the presence of ET-1-positive cerebrovascular autonomic nerves has been reported in the BA of the rat [Loesch et al., 1998; Milner et al., 2000] and of the human middle cerebral artery [Loesch and Burnstock, 2002; Mickey et al., 2002]. In the capybara BA, the presence of the endothelin A (ET_A) and B (ET_B) receptors was reported in the artery including its adventitial perivascular nerves [Loesch et al., 2005]. However, the presence of ET-1 in the perivascular nerves in capybara BA has thus far not been described.

ET-1 and its receptors ET_A and ET_B are known to be present in various structures of the nervous system, including the cerebral vessels [Edvinsson, 2009]. Neurally derived ET-1 might therefore be involved in various aspects of neurotransmission [Giaid et al., 1989; Arai et al., 1990] thereby affecting the cerebral vasculature or blood flow via autonomic perivascular nerves [Dashwood and Loesch, 2010]. However, apart from being a potent vasoconstrictor, ET-1 possesses hypertrophic, mitogenic and anti-apoptotic properties [Yanagisawa et al., 1988; Masaki et al., 1991; Nava and Lüscher, 1995; Rosendorff, 1997; Sharifi and Shiffrin, 1997].

The prime aim of this study was to investigate, qualitatively, the distribution of immunoreactive ET-1 and ET_A receptor in perivascular nerves of the BA of young and adult (maturing) capybaras using immunocytochemistry at electron-microscopic level (EM-I). Immunoreactivity for synaptophysin (SYP), an essential synaptic vesicle glycoprotein [Weidenmann and Frank, 1985; Navone et al., 1986] characteristic for functioning synapses, nerve terminals and nerve varicosities, was also examined. Structural findings by standard transmission electron microscopy (TEM) are additionally reported.

Materials and Methods

Animals

The present study was approved by the Animal Care Committee of the College of Veterinary Medicine of the University of São Paulo. Nine 6-month-old (young) females (n = 5) and males (n = 4), and nine 12-month-old (adult) females (n = 5) and males (n = 4) capybaras *(H. hydrochaeris)* were used in this study. Capybaras were obtained from the Frigorífico Panamby-Porã (Miracatu-SP), an animal breeding company licensed by the Brazilian Ministry of the Environment (license No. 182616). Capybaras were sedated by injection of 4 $mg \cdot kg^{-1}$ i.m. azaperone (Bayer, Hannover, Germany) followed by 0.06 $mg \cdot kg^{-1}$ i.m. atropine sulfate (Bayer). For anesthesia, ketamine chloride (20 $mg \cdot kg^{-1}$ i.m.) and xylazine hydrochloride (1.5 $mg \cdot kg^{-1}$ i.m.) were administered and animals were killed by an intravenous overdose (100 $mg \cdot kg^{-1}$) of thionembutal (Bayer). Via the ascending aorta, a cannula was then inserted into the left ventricle of the heart of each capybara and perfusion was initiated with a rinsing solution of 0.1 M phosphate-buffered saline (PBS; Sigma, Rochester, N.Y., USA), pH 7.4, containing 2% heparin (Roche, Rochester, N.Y., USA) and 0.1% sodium nitrite (Sigma). This was followed by perfusion with 500 ml of fixative consisting of 4% formaldehyde and 0.2% glutaraldehyde in PBS (0.1 M, pH 7.4). Brains were dissected out, and the BA isolated and placed in the same fixative for further fixation and storage (at 4–8°C) for about 1 week. All 9 adult capybaras (12–18 months old) displayed ICA regression, which appeared as a more or less advanced ligamentous cord [Reckziegel et al., 2001; Steele et al., 2006] on postmortem examination.

Standard TEM

BAs were washed in the stock PBS and then in 0.1 M (pH 7.4) sodium cacodylate buffer. Specimens were then postfixed in 1% osmium tetroxide, stained en block with 2% aqueous solution of uranyl acetate, dehydrated in a graded ethanol series followed by propylene oxide and then embedded in Araldite for polymerization. Ultrathin sections (~80 nm) of the specimens were then cut using an Ultracut E Reichert-Jung microtome equipped with a diamond knife, stained with uranyl acetate and lead citrate and subsequently examined using either a JEOL-1010 TEM or Philips-CM-120 TEM equipped with a digital camera.

EM-I of ET-1, ET_A and SYP

BAs were washed in 0.1 M PBS (Sigma, Poole, UK) containing 0.1% sodium azide and then placed in PBS at pH 7.6. Cross-sections of the BA (~100 μm thick) were cut using a vibratome (Technical Product International, Inc., St. Louis, Mo., USA), collected in PBS and processed for EM-I of ET-1, ET_A and SYP [Loesch et al., 2005; Steele et al., 2006; Loesch et al., 2010a]. Briefly, sections were exposed to 0.3% hydrogen peroxide in 33% methanol for 45 min (in

order to block endogenous peroxidases), washed in PBS and then for ET-1 detection placed for 1 h in a 10% nonimmune normal goat serum (NGS; Nordic Immunology, Tilburg, The Netherlands), while for the detection of ET_A and SYP sections were placed in a 10% nonimmune normal horse serum (NHS; Jackson ImmunoResearch Laboratories, West-Grave, Pa., USA). Sections were then exposed to avidin followed by biotin for 15 min each in order to block endogenous avidin and biotin (avidin/biotin blocking kit SP-2001; Vector Laboratories, Burlingame, Calif., USA), washed in PBS and then incubated for 48 h in one of the following antibodies: (i) a monoclonal antibody to ET-1 (diluted 1:1,000 in PBS containing 10% NGS and 0.1% sodium azide); (ii) a polyclonal antibody to ET_A (diluted 1:500 in PBS containing 10% nonimmune NHS and 0.1% sodium azide) and (c) a polyclonal antibody to SYP (diluted 1:1,000 in 10% nonimmune NHS and 0.1% sodium azide). After the antibody incubation step, sections were washed in PBS. For the detection of ET-1, sections were incubated for 4 h in a biotin-conjugated goat anti-mouse IgG serum (Jackson; diluted 1:500 in PBS containing 1% NGS and 0.1% sodium azide), while for ET_A and SYP detection sections were incubated in a biotin-conjugated donkey anti-rabbit IgG serum (Jackson; diluted 1:500 in PBS containing 1% NHS and 0.1% sodium azide). Sections were then washed in PBS, exposed to ExtrAvidin-horseradish peroxidase conjugate (Sigma) diluted 1:1,500 in PBS. The immunoreactivity was visualized with 3,3′-diaminobenzidine (Sigma). The specimens were washed in PBS and distilled water and then placed for 30 min in 1% osmium tetroxide (in 0.1 M sodium cacodylate buffer) and dehydrated in graded ethanol concentrations followed by propylene oxide. The specimens (sections) were then flat embedded in Araldite between two sheets of Melinex (Agar Scientific) and polymerized in the oven at 65°C for 12 h. The areas containing BA were cut out and then mounted on Araldite blocks for ultrathin sectioning (at 90 nm) using an Ultracut E Reichert-Jung microtome with a diamond knife; ultrathin sections were stained with uranyl acetate and lead citrate, and subsequently examined and digitally photographed at EM level using either a JEOL-1010 or Philips-CM-120 TEM.

Immunofluorescence: Laser Confocal Microscopy of SYP

Fixed BAs were washed in PBS and infiltrated overnight at 4°C with cryoprotectant consisting of 25% sucrose and 10% glycerol (by volume, in PBS). They were then embedded in OCT compound (BDH-Merk, Leicester, UK) and frozen in liquid nitrogen-cooled isopentane. Using a Leica CM1850 UV cryostat, the BAs were cross-sectioned at 30 μm and collected in PBS for the immunoprocedure. After washing for 30 min in PBS containing 0.1% Triton X-100, sections were (a) placed for 1 h in 10% nonimmune NGS (Nordic), (b) incubated for 24–48 h at room temperature in rabbit polyclonal SYP antibody (diluted 1:1,500 in PBS containing 5% nonimmune NGS, 0.1% DL-lysine and 0.1% sodium azide), (c) washed in PBS, (d) incubated for 2 h in goat anti-rabbit IgG Alexa-Fluor 488 (Invitrogen/Molecular Probes, Eugene, Oreg., USA; diluted 1:600 in PBS containing 1% nonimmune NGS, 0.1% DL-lysine and 0.1% Triton X-100), (e) washed in PBS, and then (f) mounted in anti-fade Citifluor (London, UK) for examination with a BioRad Radiance 2000 laser confocal microscope equipped with LaserSharp software; fluorescence filters allowed discrimination of labeling with a 488 excitation line. Objective lenses (×20 and ×60; both oil immersion) were used for examination of the specimens. Five consecutive individual images were collected at 3-μm intervals and then merged.

Antibodies and Immunohistochemical Controls

Well-established ET-1, ET_A and SYP antibodies were used in the present study that have previously been used in either the study of the vasculature and/or the associated autonomic nerves [Mickey et al., 2002; Loesch et al., 2005; Steele et al., 2006; Loesch et al., 2010a]. In brief, ET-1 monoclonal antibody was raised in mouse against human ET-1 (MCE-6901-01, clone IC4, isotype IgG_1; Peninsula Laboratories-Bachem UK Limited, St Helens, UK). In conjunction with anti-C-terminal it has a sensitivity of 0.06 pmol/l. ET_A affinity-purified polyclonal antibody (AER-001; Alomone Labs, Jerusalem, Israel) was raised in rabbits; it recognizes intracellular (C-terminus) epitopes corresponding to amino acid residues 413–426 of rat ET_A peptide (accession No. P26684). SYP polyclonal antibody (A010: DAKO, Glostrup, Denmark) was raised in rabbits against synthetic human SYP peptide. In the present study, the routine controls were applied for all antibodies used, with the omission of the primary antibody and IgG steps, independently, which resulted in lack of immunolabeling.

Results

Perivascular Nerves: Standard TEM

Both young and adult capybara BA showed characteristics of a cerebral artery consisting of 3 main histological layers namely the intima with its endothelium, the media with its vascular smooth muscle cells and the adventitia with its perivascular autonomic nerves (for more details, see a previous study from our laboratories: [Islam et al., 2004]).

Young Capybaras

As expected, the perivascular nerves including nerve fibers/axons were present in the adventitia of the BA in capybaras examined in this group (fig. 1a, b). Perivascular nerves appeared in bundles and singly. Axon varicosities and also axon intervaricosities were observed in the vicinity of vascular smooth muscles or in peripheral regions of the adventitia, i.e. at some distance from vascular smooth muscles (fig. 1a). The axon varicosities displayed agranular and granular vesicles as well as mitochondria (fig. 1b). Varicosities and intervaricosities were usually accompanied by Schwann cell processes.

Adult Capybaras

In addition to structurally well-preserved perivascular autonomic nerves, some nerves displayed structural abnormalities in this group. Abnormalities concerned both the Schwann cells and axon profiles (fig. 1c, d). In Schwann cells, the cytoplasm was swollen and vacuolated (fig. 1c) and/or displaying multilamellar myelin-like figures (fig. 1d). Although axons appeared more or less structurally preserved, some axon profiles were irregular in shape and their content had increased electron density compared to young animals (fig. 1d).

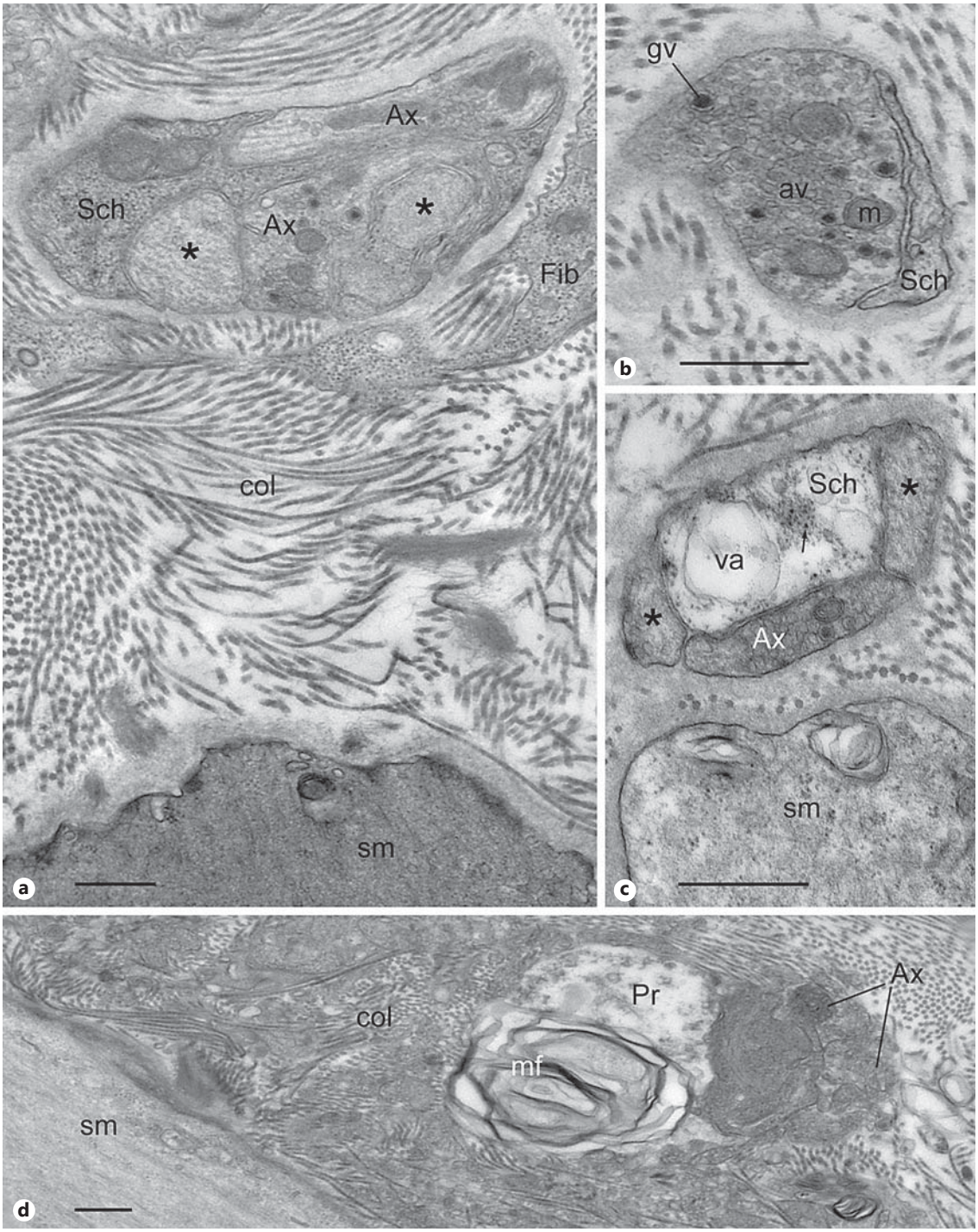

Fig. 1. Standard EM of perivascular nerves and/or perivascular structures of the BA of young (**a**, **b**) and adult (**c**, **d**) capybaras. **a**, **b** Well-structured axon varicosities (Ax) and intervaricosities (asterisks); in varicosities both granular (gv) and numerous agranular (av) vesicles are present. Schwann cell (Sch), fibroblast (Fib), collagen (col), mitochondria (m) and vascular smooth muscle (sm) can also be seen. **c** Altered nerve profile; changes are associated with the Schwann cell displaying vacuolated cytoplasm (va) and fine granular material (arrow) – possibly glycogen; also note that varicosities and intervaricosities are rather well preserved. **d** Advanced changes in perivascular structure/nerve located close to the vascular smooth muscle; in a profile (Pr), possibly a Schwann cell, a multilamellar figure (mf) is present, while axon profiles show dense cytoplasm and/or accumulated vesicles. Scale bars = 0.5 μm.

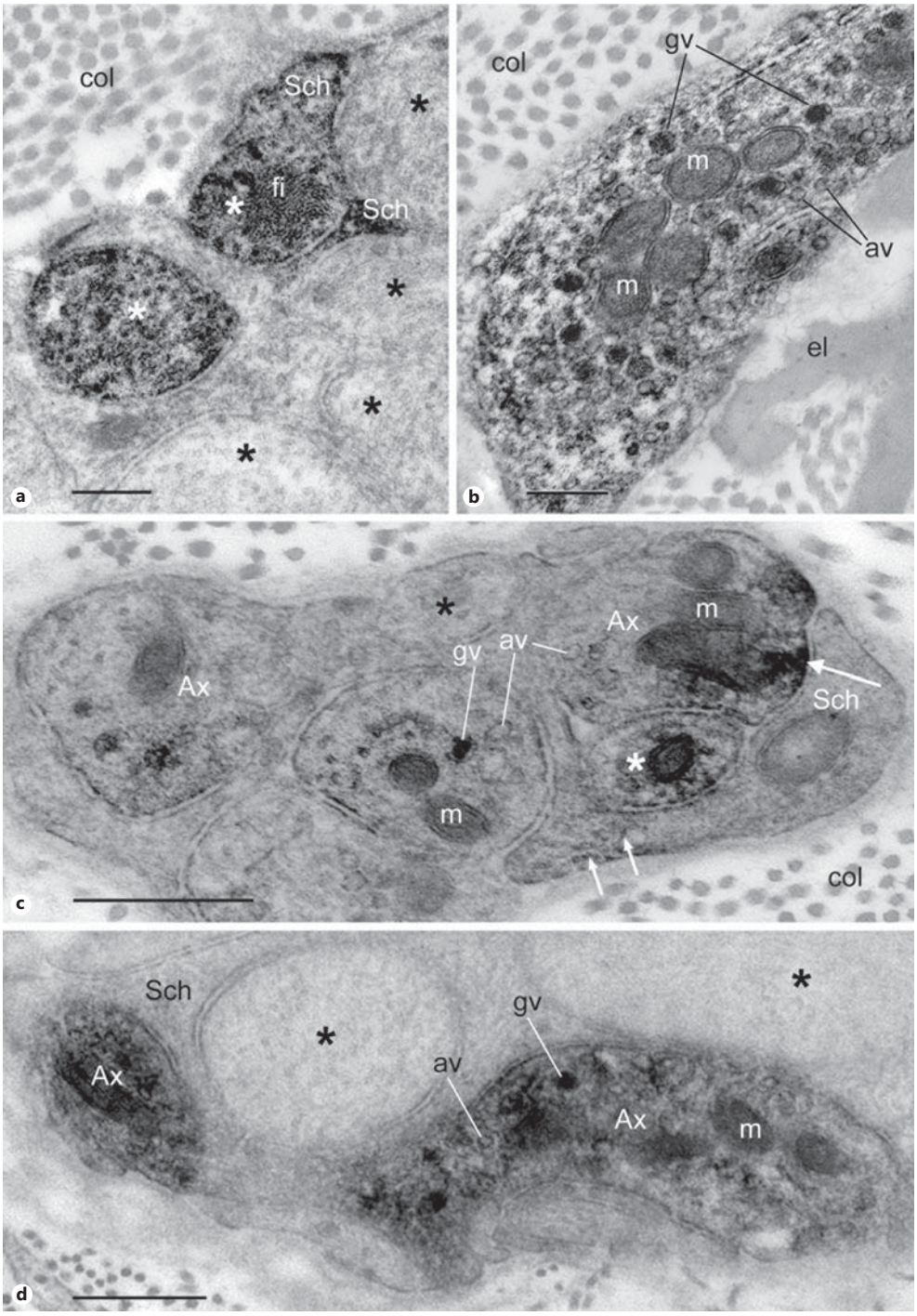

Fig. 2. EM-I of ET-1 (**a**, **b**), ET_A (**c**) and SYP (**d**) in perivascular nerves of the BA of young capybaras; black immunoprecipitate marks antigenic sites. (Note that a similar pattern of labeling for ET-1, ET_A and SYP in nerve profiles can also be observed in adult capybaras – data not shown.) **a** One of the two ET-1-positive intervaricosities (white asterisks) contains numerous filaments (fi); other visible intervaricosities are unlabeled (black asterisks). Also note ET-1-positive and ET-1-negative Schwann cell processes (Sch). Collagen (col) can also be seen. **b** Granular (gv; ~80–90 nm) and agranular (av; ~50 nm) vesicles in axon varicosity. Mitochondria (m) and elastin (el) can also be seen. **c** Immunoreactivity for ET_A is seen both in axon varicosities (Ax) and intervaricosities (white asterisks). Note substantial patch of axoplasm-located immunoreactivity (long white arrow) near the contact with a Schwann cell. **d** Immunoreactivity for SYP associates with axon varicosities but not intervaricosities, which remain unlabeled (black asterisks). Granular and agranular vesicles can be seen in labeled varicosities. **a**, **b** Scale bars = 0.25 μm. **c**, **d** Scale bars = 0.5 μm.

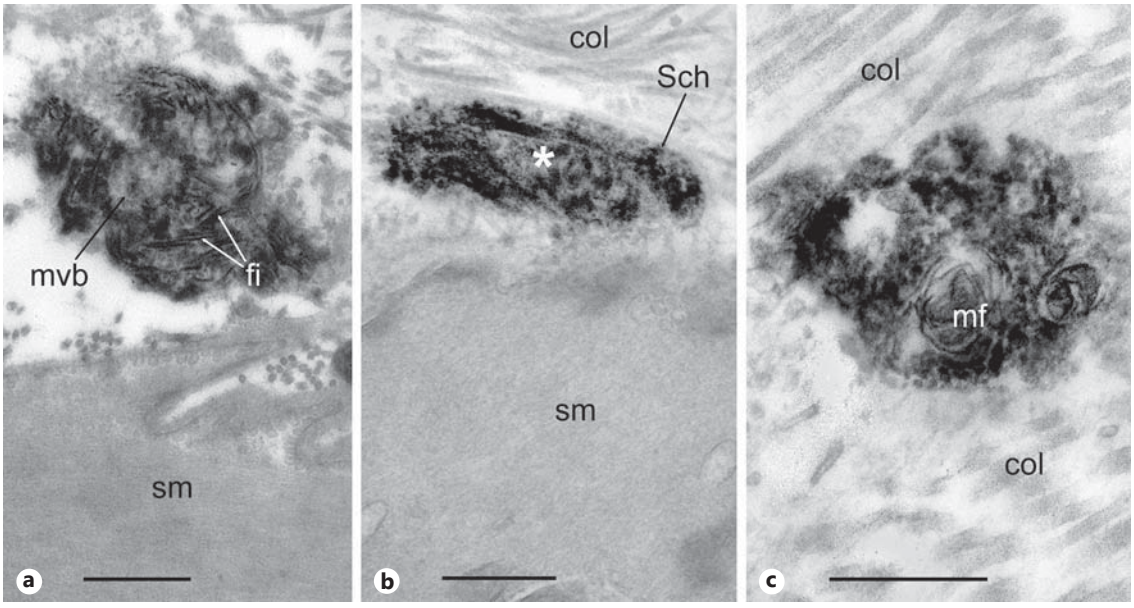

Fig. 3. EM-I of ET-1 (**a**), ET_A (**b**) and SYP (**c**) in perivascular nerves and/or 'unknown' perivascular structures of the BA of adult capybaras; black immunoprecipitate marks immunoreactive sites, respectively. In general, it is difficult to see what cell types are involved. **a** Multivesicular bodies (mvb) and filaments (fi) are seen within the ET-1-labeled structure; vascular smooth muscle (sm) is unlabeled. **b** A white asterisk marks a possible axon profile containing ET_A-labeled granular material; the axon is enclosed by ET_A-labeled Schwann cell processes (Sch). Collagen (col) can be seen. **c** Myelin-like figures (mf) within SYP-labeled structure. Scale bars = 0.5 μm.

Perivascular Nerves: EM-I of ET-1, ET_A and SYP

Young Capybaras

The application of immunocytochemistry identified the antigenic sites of ET-1 (fig. 2); these were seen as black immunoprecipitate within axon profiles including their intervaricose and varicose sites. In some ET-1-positive intervaricosities, numerous filaments were present (fig. 2a), while in ET-1-positive varicosities numerous granular and agranular vesicles (80–90 and 40–50 nm in diameter, respectively) dominated (fig. 2b). Apart from ET-1-positive axon profiles, ET-1-negative axons were also observed. The same was true for the Schwann cells, which also showed both ET-1-positive and ET-1-negative processes (fig. 2a). In general, the ET-1 label was seen on the cell membrane (axolemma), microtubules and granular vesicles in axon profiles, while in Schwann cell processes it was deposited in the cytoplasm.

Perivascular nerves of young capybaras also displayed immunoreactive ET_A receptor labeling. Immunoreactivity was discrete and seen in the axon profiles and, to a lesser extent, in accompanying Schwann cell processes (fig. 2c). In axons, both varicosities and intervaricosities were ET_A positive. In varicosities, the immunoprecipitate labeled the core of granular vesicles and other cytoplasmic structures. Patches of immunoprecipitate were present in the axoplasm, in particular at the sites of contact with the accompanied Schwann cell (fig. 2c). Some axon profiles were negative for ET_A receptors (fig. 2c).

In young capybaras, perivascular nerves appeared positive for SYP. As expected, the immunoreactive SYP was associated with axon varicosities containing both granular and agranular synaptic vesicles, while intervaricosities were unlabeled and no synaptic vesicles were present (fig. 2d). At higher magnification, immunolabeling of the membrane of some vesicles and the core of the granular vesicles was observed.

Adult Capybaras

Perivascular nerves displaying similar structural and immunocytochemical features to those described above for young capybaras were also observed in the BA of adult capybaras. However, some nerve profiles were distinctly different and displayed immunolabeling of ET-1, ET_A receptor and SYP (fig. 3). The labeled altered nerve profiles could be seen in close vicinity of vascular smooth muscles (fig. 3a, b).

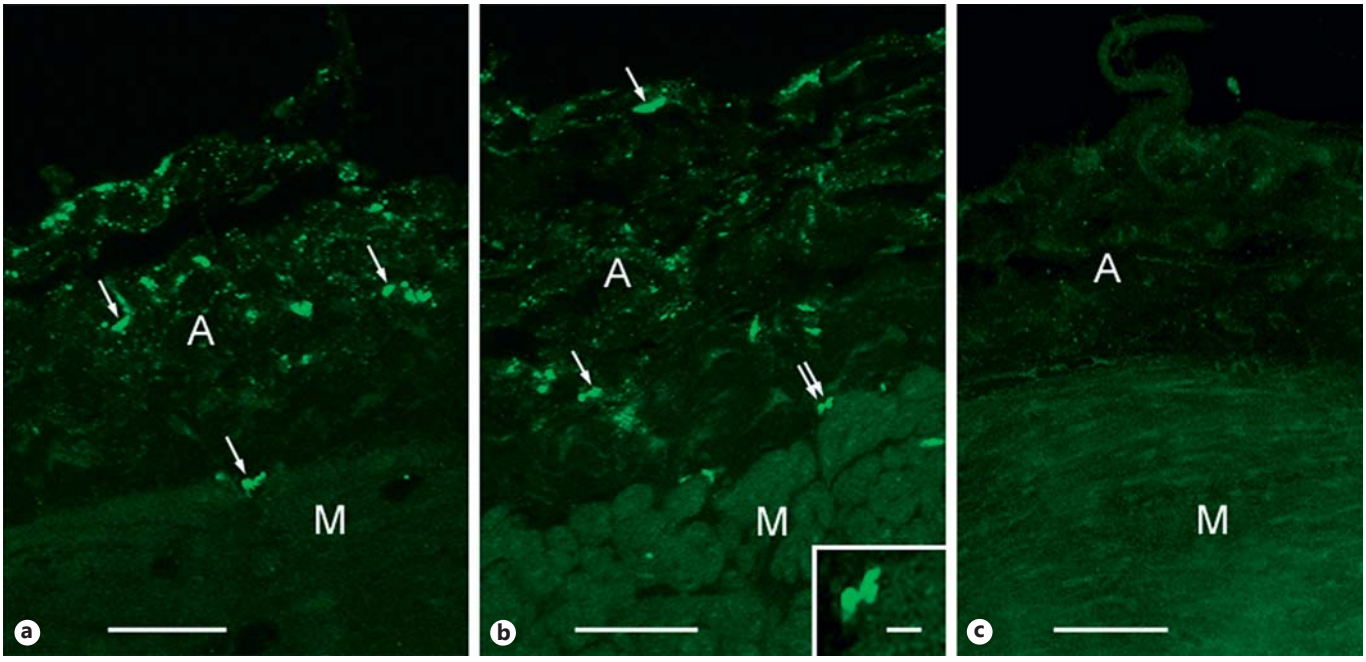

Fig. 4. Confocal immunofluorescence microscopy of BA of young (**a**) and adult (**b**) capybaras, respectively, immunolabeled for SYP (light green label in original images; arrows). **c** Negative control of the BA from 6-month-old capybara. **a**, **b** Nerve varicosities seen as punctate immunolabeling throughout the adventitia (A). M = Media. Inset: magnified region of **b** at the adventitia-media border (double arrows) showing SYP-fluorescent structure close to the media. **c** Lack of immunolabeling when SYP antibody step was omitted. Scale bars = 50 μm (inset = 5 μm).

Perivascular Nerves: Laser Confocal Immunofluorescence Microscopy of SYP

Young and Adult Capybaras

General observations with the confocal microscopy showed the presence of SYP-immunoreactive perivascular nerves in the BA of both young and adult capybaras. Immunolabeling for SYP was therefore seen throughout the adventitia as a punctate fluorescence including labeled structures located at the adventitia-media border (fig. 4a, b). No immunolabeling for SYP was seen in immunohistochemical control preparations (fig. 4c).

Discussion

This study demonstrates for the first time the presence of ET-1-positive perivascular autonomic nerves in the BA of young and adult (maturing) capybaras, as observed at EM level. Perivascular nerves also showed immunoreactivity for ET_A receptor and SYP. This study also revealed that the ET-1-positive perivascular nerves, including both axon profiles and accompanying Schwann cells, underwent changes at animal maturation coinciding with ICA regression. Our findings, therefore, supplement our previous data on the fine structure of the BA in capybaras and to the artery changes during animal maturation and ICA regression [Islam et al., 2004; Loesch et al., 2005; Steele et al., 2006]. It should be mentioned, however, that it has previously been demonstrated that in a large proportion of capybaras at maturation (which is at about 1 year of age), the ICA is no longer functioning efficiently due to the collapsed lumen, decreased lumen size and transformation to a ligamentous cord. Therefore, the BA becomes the main anatomical conduit via which blood is supplied to the brain from the vertebrobasilar system [Reckziegel et al., 2001; Steele et al., 2006]. In such circumstances, the BA can more than double its size including its luminal size/diameter e.g. from about 0.9 mm in young capybaras to about 2.2 mm in adult animals [Steele et al., 2006]. It seems reasonable, therefore, to suggest that upon such changes various components of the vascular wall might be affected.

Perivascular Nerve Structure

In young capybaras, the fine structure of perivascular nerves, consisting of axons and Schwann cells, recorded

in this study agrees with the previously observed features of cerebrovascular nerves in this animal [Islam et al., 2004] or autonomic nerves in general [Burnstock and Iwayama, 1971]. Hence the presence of characteristic both agranular and granular vesicles in axon varicosities and the appearance of Schwann cells were classic. The differences appeared upon animal maturation and ICA regression, where Schwann cells become structurally affected with cytoplasmic distortion: vacuolization and the presence of multilamellar bodies. Similar changes, e.g. cytoplasmic vacuolization, may be observed in Schwann cells in diabetic peripheral nerve pathology [Loesch et al., 2010b] or the occurrence of myelin-like figures in Wallerian-like degeneration; the latter may in fact occur without the presence of macrophages to remove debris, e.g. myelin [Fernandez-Vall et al., 1995]. By the same token, it seems possible that axonal abnormalities, including changes in axonal shape, axoplasm electron density and/or the changes in the vesicle number and appearance, as observed in adult capybaras, may be related to a degenerative process [Picklo, 1997; Said, 2007]. Therefore, the TEM studies might suggest remodeling and/or degeneration/regeneration of at least some nerve profiles in capybara BA during maturation and regression of the ICA. Changes in blood load and presumably hypertension may occur in the BA at this stage. Hypertension and diabetes are known to induce peripheral nerve neuropathy [Gregory et al., 2012], while vasospasm, even as a temporary event producing obstruction to the blood flow following subarachnoid hemorrhage, causes morphological changes in the cerebral vasculature [Mayberg et al., 1990]. Notably, in spontaneously hypertensive rats, structural changes in ET-1-positive axon varicosities in the BA were reported [Milner et al., 2000a].

EM-I

The EM-I study demonstrated that ET-1 immunoreactivity in perivascular nerves of young capybaras was similar to that previously reported in rats and humans [Loesch et al., 1998; Milner et al., 2000; Loesch and Burnstock, 2002; Mickey et al., 2002]. Such results also agree with the demonstration of binding sites for ET-1 on perivascular nerves of various blood vessels in humans [Dashwood et al., 1996; Dashwood and Thomas, 1997; Dashwood et al., 1998, 2000]. In capybara BAs, the ET-1-immunoprecipitate labeled predominantly membranous structures and the core of granular vesicles. The immunoreactive sites of the ET_A receptor were less evenly distributed and at times accumulated in the axoplasm at the axon-Schwann cell contact. However, in axon profiles also, the core of granular vesicles may be ET_A labeled. Again, this 'uneven' ET_A labeling seems normal for capybara cerebrovascular nerves [Loesch et al., 2005]. However, in the capybaras with regressed ICA (and hence changes in blood supply to the brain), heavy labeling for ET-1, ET_A receptor and SYP was also related to perivascular nerves displaying an abnormal ultrastructure. It is unknown if these phenomena result from an increased production and increased expression of ET-1, ET_A and SYP in perivascular nerves. Alternatively, this may reflect an inhibition of turnover of ET-1, ET_A and SYP and subsequent accumulation of these 'redundant' molecules at this stage.

However, the most intriguing phenomenon is the strong expression of immunoreactivity for SYP in the evidently distorted or possibly even remnants of perivascular nerves. In normal circumstances, SYP is exclusively associated with functional synapses, as SYP is an integral membrane protein (glycoprotein) of synaptic vesicles [Weidenman and Frank, 1985; Navone et al., 1986; Tarsa and Goda, 2002]. Interestingly, no axon varicosities showing immunoreactive SYP were present in the regressed ICA (in ICA-ligamentous cord) of 1-year-old capybaras, but in contrast in the ICA of young (6-month-old) animals, SYP was detected in the axon varicosities [Steele et al., 2006]. Whether the SYP-positive and structurally altered nerve profiles in the BA undergo degeneration and discontinue their normal function is not clear at this stage. The possibility cannot be excluded that non-neural cells are also involved, e.g. macrophages [Liu, 1974]. Alternatively, these features of altered perivascular nerves might represent 'apparent degeneration' followed by perivascular nerve recovery, as can be observed in diabetic autonomic neuropathy for example [Monckton and Pehowich, 1980]. Notably, it has been reported that the BA of 1-year-old capybara showed some 'unusual' vascular smooth muscle described as 'granular', which suggested a remodeling process in the artery at this animal age, when ICA regression occurs [Islam et al., 2004].

Role of ET-1 and ET_A Receptor in the Cerebral Vascular Bed

One of the questions raised by the results of this study regards the possible role that ET-1-positive perivascular nerves may play in the BA and/or cerebrovascular bed. The possibility that neural ET-1 released from cerebrovascular nerves may play a physiological role [Milner et al., 2000] is now strengthened by the evidence that the ET_A receptor is also associated with these nerves. In fact, we have previously reported on the presence of immunoreactive ET_A and ET_B receptors in the perivascular nerves

of capybara BA, but it was not clear if the BA nerves also expressed immunoreactive ET-1 [Loesch et al., 2005]. The present study shows that some nerves were indeed ET-1 immunoreactive. It should be mentioned, however, that in capybara BA ET-1 and its receptors are also associated with intimal endothelium, adventitial fibroblasts and medial vascular smooth muscle [Loesch et al., 2005].

To date, immunoreactive ET-1 in cerebrovascular nerves has been reported in rat and human cerebral vessels [Loesch et al., 1998; Milner et al., 2000a; Loesch and Burnstock, 2002; Mickey et al., 2002; Loesch, 2003]. Data on the rat suggest that about 36% of perivascular axon profiles in the BA may express ET-1 [Loesch et al., 1998]. As our study did not set out to be quantitative, e. g. assessing the density or proportion of ET-1- and ET_A-positive nerves with immunofluorescence methodology, the quantity of ET-1-positive perivascular nerves in capybara BA is unknown at this stage. Our attempts to perform quantitative analysis failed [our unpubl. pilot study] as we observed that both ET-1 and ET_A antibodies produced inconclusive immunofluorescence results (most likely this was due to the cross-linkage of tissue proteins upon aldehyde fixation). Therefore, the emphasis of the present study was on the ultrastructural and immunocytochemical characteristics of perivascular nerves labeled with ET-1, ET_A and SYP antibodies with the preembedding ExtrAvidin-peroxidase protocol for EM. Nonetheless, these nerves appeared less frequently in capybaras than rats [Loesch et al., 1998]; hence, ET-1-positive nerves were lacking in our previous study of the capybara BA [Loesch et al., 2005]. The most likely main source of the ET-1-containing cerebrovascular nerves, at least in the rat, is the sensory trigeminal ganglion, as has been established in experiments with sensory or sympathetic denervation and in situ hybridization [Milner et al., 2000b]. The current finding of ET-1-positive cerebrovascular nerves as well as the presence of ET_A and also ET_B receptors in the nerves of the capybara BA [Loesch et al., 2005] strengthens the suggestion that these are indeed functional nerves possibly involved in cerebral vasoconstriction.

Pharmacological studies showed that ET-1 is a potent vasoconstrictor of the cerebral vascular bed [Kobayashi et al., 1990] and that this phenomenon is linked with the presence of ET_A receptors [Adner et al., 1993; Zimmermann and Seifert, 1998]. Studies of cerebral arteries of various mammals showed that alongside the contractile ET_A receptor, the pharmacologically active dilatory ET_B receptor may be present [Patel et al., 1996; Yakubu and Leffler, 1996, Zimmermann and Seifert, 1998]. Likewise, the contractile ET_A and dilatory ET_B receptors and their mRNAs have also been reported in human cerebral arteries, where the mRNAs were identified in the presence or absence of the intimal endothelium [Nilsson et al., 1997]. In human blood vessels, both ET_A and ET_B receptors are involved in ET-1-mediated contraction [Seo et al., 1994]. However, there may also be an additional role for ET-1 and ET_A receptors, namely an involvement in the interaction with Schwann cells. In this context, ET-1-positive Schwann cells embracing ET-1-negative and/or ET-1-positive perivascular axon profiles were noted in the human middle cerebral artery in a case of multiple system atrophy with autonomic failure [Loesch et al., 2004].

In conclusion, EM-I results showed that ET-1 and ET_A receptors are present in some perivascular autonomic nerves of the BA of young capybaras and that these, together with accompanying Schwann cells, might undergo changes during animal maturation, when the ICA regresses. Therefore, the observed changes are likely to be a part of BA remodeling due to altered blood supply to the brain. It would be interesting to investigate further if there is a colocalization of ET-1 and ET_A receptors with other vasoactive agents and their receptors in conjunction with pharmacological studies. Although these are preliminary studies of the capybara brain and cerebral vasculature, it might be of interest to consider the capybara as a naturally occurring animal model to investigate the remodeling of the cerebral vasculature and cerebral blood flow, and also to study various hemodynamic conditions associated with cerebral ischemia and stroke (due to BA overload at ICA regression).

Acknowledgments

Support by the São Paulo Research Foundation (FAPESP; application: 2009/53545-9) is greatly acknowledged (A.A.C. – the Laboratory of Stochastic Stereology and Chemical Anatomy). M.R.D. wishes to thank Dr Michael Thomas for financial support. A.L. is grateful for the research environment provided by the Center for Amyloidosis and Acute Phase Proteins, Division of Medicine, Royal Free Campus, UCL, London, UK.

References

Adner, M., J. You, L. Edvinsson (1993) Characterization of endothelin A receptors in the cerebral circulation. Neuroreport *4:* 441–443.

Arai, H., S. Hori, I. Aramori, H. Ohkubo, S. Nakanishi (1990) Cloning and expression of a cDNA encoding an endothelin receptor. Nature *348:* 730–732.

Burnstock, G. (1988) Regulation of local blood flow by neurohumoral substances released from perivascular nerves and endothelial cells. Acta Physiol Scand *133:* 53–59.

Burnstock, G. (1990) Local mechanisms of blood flow controlled by perivascular nerves and endothelium. J Hypertens *8:* S95–S106.

Burnstock, G., T. Iwayama (1971) Fine structural identification of autonomic nerves and their relation to smooth muscle. Progr Brain Res *34:* 389–404.

Dashwood, M.R., A. Loesch (2010) Endothelin-1 as a neuropeptide: neurotransmitter or neurovascular effects? J Cell Commun Signal *4:* 51–62.

Dashwood, M.R., P.K. Thomas (1997) Neurovascular [^{125}I]-ET-1 binding sites on human peripheral nerve. Endothelium *5:* 119–123.

Dashwood, M.R., M. Timm, J.C. Kaski, A.J. Murday, B.P. Madden (1996) [^{125}I]-ET-1 binding to perivascular nerves of human epicardial coronary arteries. Endothelium *4:* 231–234.

Dashwood, M.R., G.D. Angelini, D. Mehta, J.Y. Jeremy, M. Muenter, M. Kirchengast (1998) Effect of angioplasty and grafting on porcine vascular nerves: a potential neurotropic role for endothelin-1. J Anat *192:* 435–437.

Dashwood, M.R., R. Gibbins, D. Mehta, M. Bashar Izzat, G.D. Angelini, J.Y. Jeremy (2000) Neural reorganisation in porcine vein grafts: a potential role for endothelin-1. Atherosclerosis *150:* 43–53.

De Vriese, B. (1905). Sur la signification morphologique des artères cérébrales. Arch Biol *21:* 357–457.

Edvinsson, L. (2009) Cerebrovascular endothelin receptor upregulation in cerebral ischemia. Curr Vasc Pharmacol *7:* 26–33.

Faraci, F.M., J.E. Brian, Jr. (1994) Nitric oxide and the cerebral circulation. Stroke *25:* 692–703.

Fernandez-Valle, C., R.P. Bunge, M.B. Bunge (1995) Schwann cells degrade myelin and proliferate in the absence of macrophages: evidence from in vitro studies of Wallerian degeneration. J Neurocytol *24:* 667–679.

Giaid, A., S.J. Gibson, N.B.N. Ibrahim, S. Legon, S.R. Bloom, M. Yanagisawa, T. Masaki, I.M. Varndell, J.M. Polak (1989) Endothelin-1, an endothelium-derived peptide, is expresssed in neurons of the human spinal cord and the dorsal root ganglia. Proc Natl Acad Sci USA *86:* 7634–7638.

Gregory, J.A., C.G. Jolivalt, J. Goor, A.P. Mizisin, N.A. Calcut (2012) Hypertension-induced peripheral neuropathy and the combined effects of hypertension and diabetes on nerve structure and function in rats. Acta Neuropathol *124:* 561–573.

Herrera, E.A., D.W. Macdonald (1984) The capybara; in D.W. Macdonald (ed): Encyclopaedia of Mammals. London, Allen & Unwin, pp 696–699.

Islam, S., A.A.C.M. Ribeiro, A. Loesch (2004) Basilar artery of the capybara *(Hydrochaeris hydrochaeris)*: an ultrastructural study. Anat Histol Embryol *33:* 81–89.

Kobayashi, H., M. Hayashi, S. Kobayashi, M. Kabuto, Y. Handa, H. Kawano (1990) Effect of endothelin on the canine basilar artery. Neurosurgery *27:* 357–361.

Liu, H.M. (1974) Schwann cell properties. II. The identity of phagocytes in the degenerating nerve. Am J Pathol *75:* 395–416.

Loesch, A. (2003) Nitric oxide synthase and endothelin in cerebrovascular nerves of the basilar artery in pregnant rat. Biomed Res (India) *14:* 1–5.

Loesch, A., G. Burnstock (2002) Endothelin in human cerebrovascular nerves. Clin Sci *103(suppl 48):* 404S–407S.

Loesch, A., P. Milner, G. Burnstock (1998) Endothelin in perivascular nerves. An electron-immunocytochemical study of rat basilar artery. Neuroreport *9:* 3903–3906.

Loesch, A., L. Kilford, A. Kingsbury (2004) Endothelin in Schwann cells of middle cerebral artery in multiple system atrophy case. Biomed Res (India) *15:* 157–159.

Loesch, A., B. Gajkowska, M.R. Dashwood, E.T. Fioretto, K.M. Gagliardo, A.R. de Lima, A.A.C.M. Ribeiro (2005) Endothelin-1 and endothelin receptors in the basilar artery of the capybara. J Mol Histol *36:* 25–34.

Loesch, A, T.M. Mayhew, H. Tang, F.V. Lobo Ladd, A.A.B. Lobo Ladd, M.P. de Melo, A.A.P. da Silva, A.A. Coppi (2010a) Stereological and allometric studies on neurons and axo-dendritic synapses in the superior cervical ganglia of rats, capybaras and horses. Cell Tissue Res *341:* 223–237.

Loesch, A., H. Tang, M.A. Cotter, N.E. Cameron (2010b) Sciatic nerve of diabetic rat treated with epoetin delta: effects on C-axons and blood vessels including pericytes. Angiology *61:* 651–668.

Masaki, J., S. Kimura, M. Yanagisawa, K. Goto (1991) Molecular and cellular mechanisms of endothelin regulation. Implications for vascular function. Circulation *84:* 1457–1468.

Mayberg, M.R., T. Okada, D.H. Bark (1990) Morphologic changes in cerebral arteries after subarachnoid hemorrhage. Neurosurg Clin N Am *2:* 417–432.

Mickey, I., L. Kilford, A. Kingsbury, A. Loesch (2002) Endothelin in the middle cerebral artery: a case of multiple system atrophy. Histochem J *34:* 469–477.

Milner, P., A. Loesch, G. Burnstock (2000a) Neural endothelin in hypertension: increased immunoreactivity in ganglia and nerves to cerebral arteries of the spontaneously hypertensive rat. J Vasc Res *37:* 39–49.

Milner, P., A. Loesch, G. Burnstock (2000b) Endothelin immunoreactivity and mRNA expression in sensory and sympathetic neurones following selective denervation. Int J Devl Neurosci *18:* 727–734.

Monckton, G., E. Pehowich (1980) Autonomic neuropathy in the streptozotocin diabetic rat. Can J Neurol Sci *7:* 135–142.

Nava, E., T.F. Lüscher (1995) Endothelium-derived vasoactive factors in hypertension. Nitric oxide and endothelin. J Hypertens Suppl *13:* S39–S48.

Navone, F., R. Jahn, G. Di Gioia, H. Stuckenbrok, P. Greengard, P. De Camilli (1986) Protein p38: an integral membrane protein specific for small vesicles of neurons and neuroendocrine cells. J Cell Biol *103:* 2511–2527.

Nilsson, T., L. Cantera, M. Adner, L. Edvinsson (1997) Presence of contractile endothelin-A and dilatory endothelin-B receptors in human cerebral arteries. Neurosurgery *40:* 346–351.

Patel, T.R., M.A. McAuley, J. McCulloch (1996) Endothelin receptor mediated constriction and dilatation in feline cerebral resistance arterioles in vivo. Eur J Pharmacol *307:* 41–48.

Picklo, M.J. (1997) Methods of sympathetic degeneration and alteration. J Auton Nerv Syst *62:* 111–125.

Ralevic, V., G. Burnstock (1993) Neural-Endothelial Interactions in the Control of Local Vascular Tone. Austin, Landes.

Reckziegel, S.H., T. Lindemann, R. Campos (2001) A systematic study of the brain base arteries in capybara *(Hydrochoerus hydrochaeris)*. Braz J Morphol Sci *18:* 103–110.

Rosendorff, C. (1997) Endothelin, vascular hypertrophy, and hypertension. Cardiovasc Drugs Ther *10:* 795–802.

Saetrum Opgaard, O., S. Gulbenkian, L. Edvinsson (1998) Neurovascular interactions; in J.M. Polak (ed): Modern Visualisation of the Endothelium. Amsterdam, Harwood Academic, pp 59–91.

Said, G. (2007) Diabetic neuropathy – a review. Nat Clin Pract Neurol *3:* 331–340.

Seo, B., B.S. Oemar, R. Siebenmann, L. von Segesser, T.F. Lüscher (1994) Both ETA and ETB receptors mediate contraction of endothelin-1 in human blood vessels. Circulation *89:* 1203–1208.

Sharifi, A.M., E.L. Shiffrin (1997) Apoptosis in aorta of deoxycorticosterone acetate-salt hypertensive rats: effect of endothelin receptor antagonism. J Hypertens *15:* 1441–1448.

Steele, C., E.T. Fioretto, T.H.C. Sasahara, W.I. Guidi, A.R. de Lima, A.A.C.M. Ribeiro, A. Loesch (2006) On the atrophy of the internal carotid artery in capybara. Cell Tissue Res *326:* 737–748.

Tarsa, L., Y. Goda (2002). Synaptophysin regulates activity-dependent synapse formation in cultured hippocampal neurons. Proc Natl Acad Sci USA *99:* 1012–1016.

Weidenman, B., W.W. Frank (1985) Identification and localization of synaptophysin, an integral membrane glycoprotein of Mr 38,000 characteristic of presynaptic vesicles. Cell *41:* 1017–1028.

Yakubu, M.A., C.W. Leffler (1996). Role of endothelin-1 in cerebral hematoma-induced modification of cerebral vascular reactivity in piglets. Brain Res *734:* 149–156.

Yanagisawa, M., H. Kurihara, S. Kimura, Y. Tomobe, M. Kobayashi, Y. Mitsui, Y. Yasaki, K. Goto, T. Masaki (1988) A novel potent vasoconstrictor peptide produced by vascular endothelial cells. Nature *333:* 411–415.

Zimmermann, M., V. Seifert (1998) Endothelin and subarachnoid hemorrhage: an overview. Neurosurgery *43:* 863–876.